International Journal of Science and Research Archive
eISSN: 2582-8185
Cross Ref DOI: 10.30574/ijsra
Journal homepage: https://ijsra.net/

(RESEARCH ARTICLE)

Check for updates

Thickness-dependent plasma polymerized N-Vinyl-2-Pyrrolidone Thin Films: investigation of structural and optical properties

S Mridul Kanti Saha [1, 2, *], Syed Jamal Ahmed [1] and ATM Kaosar Jamil [1]

[1] *Department of Physics, Faculty of Science, Dhaka University of Engineering & Technology, Gazipur, Bangladesh.*
[2] *Department of Electrical and Electronic Engineering, Faculty of Science & Engineering, Gono Bishwabidyalay, Bangladesh.*

International Journal of Science and Research Archive, 2025, 14(03), 1200-1210

Publication history: Received on 11 February 2025; revised on 18 March 2025; accepted on 21 March 2025

Article DOI: https://doi.org/10.30574/ijsra.2025.14.3.0789

Abstract

Plasma polymerized N-Vinyl-2-Pyrrolidone (PPNVP) thin films of different thicknesses are prepared onto glass substrates at room temperature under the pressure of 60 torr by capacitively coupled AC glow discharge plasma system. Fourier Transform Infrared Spectroscopy (FTIR), Field-Emission Scanning Electron Microscopy (FESEM), Energy Dispersive X-Ray (EDX) Spectroscopy, and Ultraviolet-Visible (UV-Vis) Spectroscopy are used to obtain thickness-dependent structural, morphological, elemental, and optical properties of PPNVP thin films. The IR spectrum at higher thicknesses of these films indicated small but significant increases in the C-H stretching (2976-2982 cm^{-1}) and decreases in the C-H bending (1462-1460 cm^{-1}) regions. Moreover, the peaks of the hydroxyl group (3662 and 3656 cm^{-1}) are most important for thicker films, which give rise to very unique band profiles. According to FESEM, the polymeric structure of PPNVP thin films displays frequent cleavage-type fracture and indicates the presence of hydrophilic functional groups. The EDX results show that as the thickness of the film increased, the mass (%) of carbon and nitrogen increased, while the mass (%) of oxygen decreased. Based on the results of the UV-Visible spectroscopy, the optical absorbance of all the PPNVP thin films increases sharply in the UV region, peaks at around 300 nm, and then rapidly decreases up to around 350 nm. The direct (3.23-2.98 eV) and indirect (2.77-2.62 eV) band gaps get narrower as the thickness of a thin film increases, which is characterized by structural variation with film thickness.

Keywords: Plasma polymerization; N-Vinyl-2-Pyrrolidone; FTIR; FESEM; EDX; UV-Vis spectroscopy

1. Introduction

Plasma polymerization is becoming an increasingly popular approach to synthesize new types of materials processing. It refers to the formation of thin films in the plasmas of organic monomers. Most inorganic compounds as well as conventional polymers are very different from the organic polymer produced by plasma polymerization. For forming a conventional polymer, at least several steps are required, whereas plasma polymerization needs only one step to form plasma polymerized material [1]. Plasma polymerized (PP) thin films have noteworthy advantages due to the reduced amounts of materials used, faster processing times, and the ability to modify the surface while preserving the structural properties of the bulk [2]. Industrialization of polymer thin films prepared by the plasma polymerization technique is preferable because of very good coating adhesion on almost all substrates, thermal, mechanical, and chemical stability, high barrier effects, cross-linked, insoluble, and pinhole-free characteristics [3].

The structural, optical, and electrical properties of PP thin films are mostly affected by changing carbon bonds in the film's chemical structure due to deposition time, flow rate of monomer, film thickness, and discharge power [4-6]. The films resulting from the plasma polymerization of NVP exhibit hydrophilic properties, a smooth surface, and a morphologically homogeneous appearance. The manipulation of controlled plasma characteristics, such as power and monomer flow rate, enables the customization of polymer composition and surface properties [7]. Recently, a poly N-

---

[*] Corresponding author: S Mridul Kanti Saha

Copyright © 2025 Author(s) retain the copyright of this article. This article is published under the terms of the Creative Commons Attribution Liscense 4.0.

Vinyl-2-pyrrolidone (PVP), also known as a conventional polymer nanocomposite with an amide-imide/aluminium oxide structure, was synthesized, and its chemical structure, surface appearance, and thermal stability were investigated in detail [8]. The NVP monomer is characterized by the presence of a polar amide group, which imparts hydrophilic and polar characteristics to the molecule. Another thing that makes the monomer hydrophobic is that it has methylene and methane groups in both its main and side chains. This makes it easier to make surface-active polymers [9]. PVP is utilized in the kinetically controlled synthesis of metal nanocrystals due to the desirable mild reducing power of long-chain alcohols [10].

Polymers that are based on NVP have been utilized in various fields such as plasma substitutes, soluble drug carriers, and UV-curable bio adhesives. So, NVP was chosen as a precursor in this study because it is biocompatible, non-toxic, chemically stable, and has adhesive properties [11]. Therefore, the various thicknesses of the PPNVP thin films are produced by a capacitively coupled plasma polymerization technique to study their structural and optical properties. Thus, this study will help us to find applicability of the PPNVP in different devices in optoelectronic technology.

2. Experiment Details

2.1. Monomer: N-Vinyl-2-Pyrrolidone

The monomer N-Vinyl-2-Pyrrolidone (NVP) is an organic compound, consisting of a 5-membered lactam linked to a vinyl group, used as a precursor in this research. The monomer was collected from Merck life science private limited, India.

2.2. Experimental Setup

Fig. 1 shows the schematic of the experimental setup used for the preparation of PPNVP film. This setup contains vacuum chamber, rotary pump, high voltage power supply, electrodes, high voltage probe and current probe, digital oscilloscope, spectrophotometers, ceramic substrate stand with substrate holder and cylindrical glass tube (Bell jar).

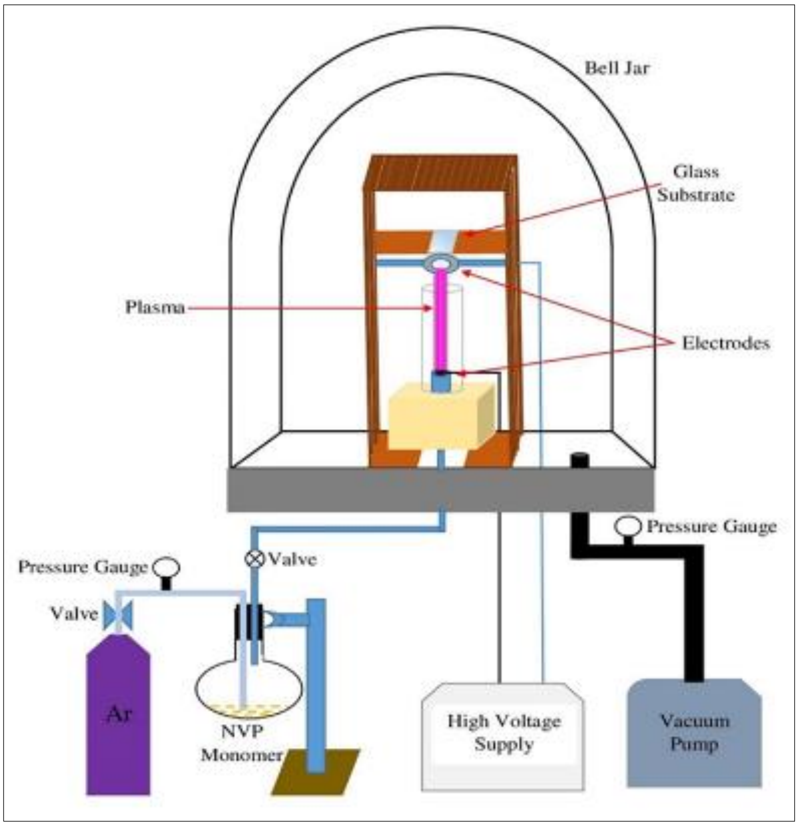

Figure 1 Schematic diagram of AC glow discharge plasma polymerization set up

2.3. Film Preparation

A (40×25) mm Pyrex glass substrate was placed at the substrate holder, and the setup was enclosed with a bell jar. We reduced the inside pressure of the bell jar five times and maintained it at 60 torr. We allowed the rotary pump to operate throughout the entire film preparation period. We connected a 15kV, 50Hz power supply across the electrodes to keep the plasma inside the glass tube. We then created plasma between the electrodes and surrounded the tube with it. We used argon gas as a carrier gas to transport the liquid NVP monomer into the bell jar. When the container's stop cock was opened, the pressure inside dropped, causing the NVP monomer to start escaping. At a rate of 0.75mL/min, PPNVP vapor began to flow into the discharge region. Subsequently, the plasma discharge color was changed due to the presence of PPNVP vapor in the discharge zone. Discharge voltage and current were measured with a high voltage and current probe in combination of an oscilloscope in order to determine plasma discharge power. We used two spectrophotometers. The electrical power (W) deposited in the discharge was ~16W.

2.4. Thickness Measurement

Thickness measurement is the most significant parameter for thin film deposition to characterize different properties of PPNVP thin film. The deposition time was varying in order to investigate the varying thickness, which forms on glass substrate at constant glow discharge power of 16 W. We used a surface Profilometer (DEKTAK 150 Profilometer) to measure the thickness of the deposited film. We prepared three thin film samples for the thickness measurement investigation, varying their times from 30, 45, and 60 minutes. Table 1 clearly shows that the film thickness increases appropriately as the deposition time increases.

Table 1 Different film thickness with varying deposition time

Deposition Time (min)	Film Thickness (nm)
30	209
45	220
60	241

---

3. Results and discussion

3.1. FTIR Analyses

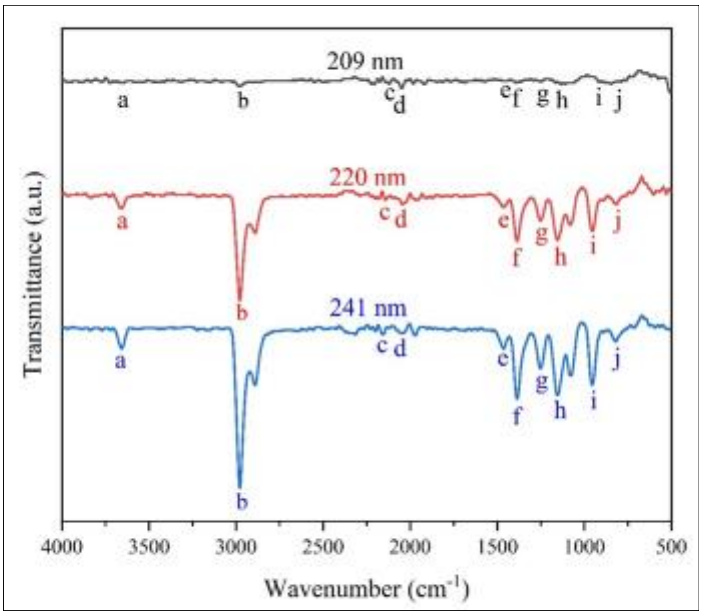

Figure 2 The FTIR spectra of PPNVP thin films of thicknesses 209 nm (black line), 220 nm (red line), and 241 nm (blue line)

The FTIR spectra for the PPNVP thin films of thicknesses 209, 220, and 241 nm are shown in Fig. 2. The corresponding absorption bands are summarized in Table 2, respectively. It is demonstrated that structural changes occur as a result of plasma polymerization and the structure of PPNVP differs moderately from that of the conventional PVP structure [7] in regard to a number of chemical bands as well as the intensity of the peaks. In the PPNVP thin films of 220 and 241 nm thickness, the absorption peaks at 3662 and 3656 cm^{-1} are assigned to hydroxyl O−H stretching and N−H stretching, respectively. The hydroxyl group primarily dominates this region, leading to the formation of distinctive band profiles. But there is no O−H stretching, and N−H stretching appears at 3662 cm^{-1} for 209 nm thickness. This could potentially be attributed to the short-time plasma treatment used to prepare this thin film.

Table 2 Peak assignments of FTIR transmittance spectra for three different PPNVP thin films and PVP monomer

Label	Assignments	Wavenumber (cm^{-1})				Intensity
		PPNVP thin film thickness			PVP [7]	
		209 nm	220 nm	241 nm		
a	N−H stretching in amine/O−H stretching in alcohol	3662	3662	3656	3459	m to s
b	C−H stretching in alkane	2976	2980	2982	2952	s to m
c	C≡N stretching in nitrile	2121	2141	2162	-	w
d	C−H bending in aromatic compound	2046	2040	2046	-	w
e	C−H bending in alkane	-	1462	1460	1461	m
f	C−H bending in alkane	-	1390	1388	1374	m
g	C−N stretching in amine	-	1252	1253	1287	m
h	C−C stretching in ring modes	1146	1150	1150	1169, 1050	m
i	C=C bending in alkene	-	953	954	-	m, broad
j	C=C bending in alkene	797	817	824	-	w

A broad O−H stretching peak is also present in the conventional polymer, but this is centered at a significantly lower wavenumber (3460 cm^{-1}) and is attributed to the presence of water contamination in the conventional polymer. The weak but reproducible peak at 2150 cm^{-1} in the PPNVP spectrum is assigned to the nitrile group (C≡N) and may result from ring-breaking reactions. Similar observations have been noted in the plasma polymerization of other nitrogen-containing monomers. The appearance peak around 2046 cm^{-1} for C−H bending in aromatic compounds is also considered to be the plasma polymerization rather than a conventional polymer. The spectrum intensity at higher thickness films significantly increases in the C−H stretching (2980−2982 cm^{-1}) and decreases in the C−H bending (1462−1460 cm^{-1}) regions. We consistently observed these spectral differences when preparing films at varying thicknesses. It is also observed that the peak position of C−H stretching shifts to the higher wavenumber region with the increase in film thickness, but C−H bending shifts almost constantly, as does the intensity. The absorption band observed at 1250 cm^{-1} arises due to C-N stretching in amine for the spectra of PVP and PPNVP films. In the spectrum for PVP, the presence of absorption band C−C stretching is observed at 1050 and 1169 cm^{-1} [7] but this absorption band is observed at around 1150 cm^{-1} for PPNVP thin films. In the spectrum for PPNVP, the presence of the absorption band C=C bending are observed at 954−797 cm^{-1} whereas this absorption band is not found in these regions for the spectrum of PVP.

Based on what has been said so far, it is clear that the PPNVP films have an aromatic ring structure with bands that stretch and bend, including O-H, C-H, C-N, C-C, and C-C. These bands are slightly shifted to a higher wavenumber region and get stronger as the film thickness increases. This phenomenon could be attributed to the increased cross-linking density in the PPNVP thin films at higher thicknesses. The above-mentioned absorption bands are very close to those of conventional PVP [7].

3.2. FESEM Analyses

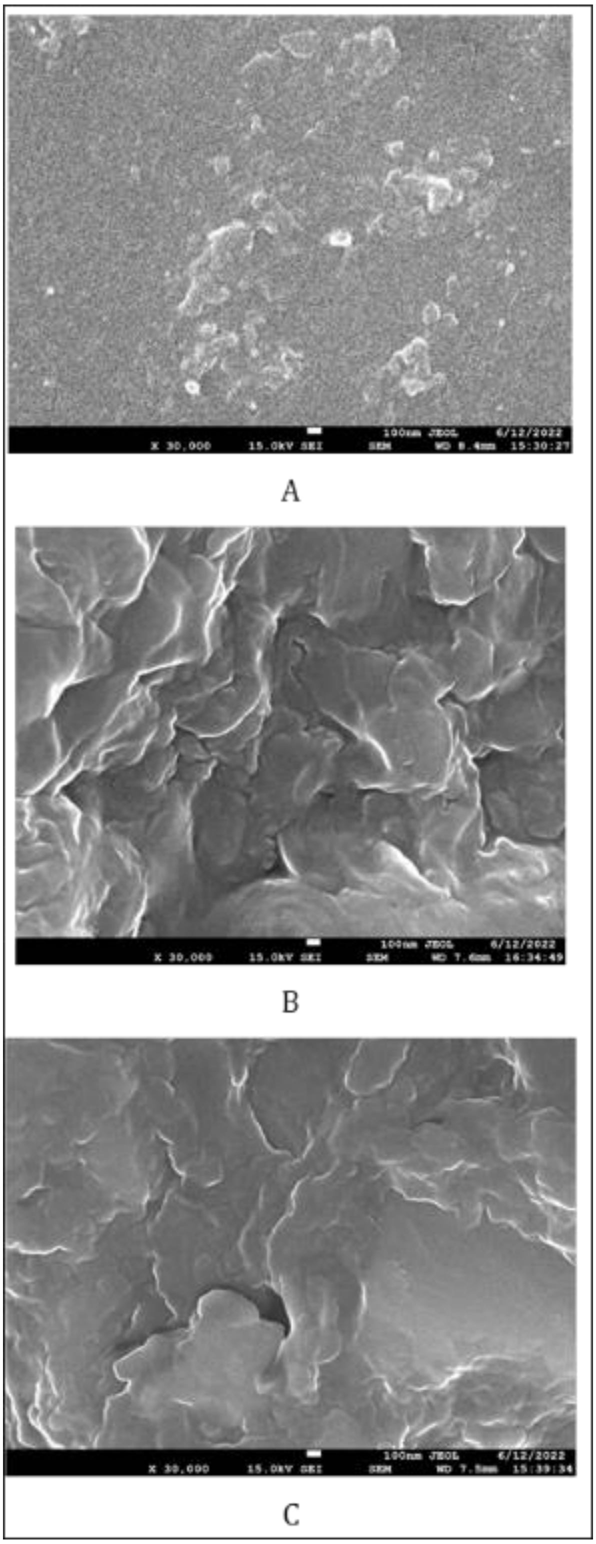

Figure 3 FESEM micrographs of PPNVP thin films with thicknesses (a) 209 nm, (b) 220 nm, and (c) 241 nm for 30,000 magnifications at accelerating voltage of 15 Kv

There are three different thicknesses of PPNVP thin films shown in Fig. 3 and 4. They are 209, 220, and 241 nm. We obtained these micrographs at various points and magnifications, approximately 30k and 50k, using an accelerating voltage of 15 kV. The PPNVP thin films exhibit a primarily cleavage-type structure on their surfaces at higher thickness.

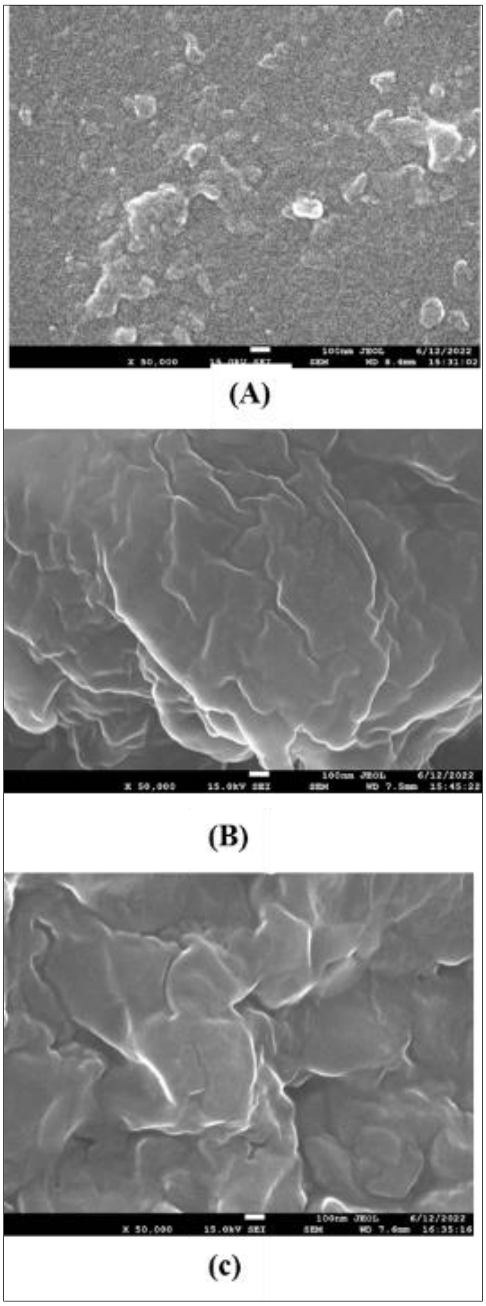

Figure 4 FESEM micrographs of PPNVP thin films with thicknesses (a) 209 nm, (b) 220 nm, and (c) 241 nm for 50,000 magnifications at accelerating voltage of 15 kV

Two factors may contribute to this type of appearance. Firstly, PPNVP is a hydrophilic polymer that undergoes rearrangement and swelling during plasma polymerization, resulting in an increase in size at multiple times compared to its dry size [12]. Secondly, the plasma treats films with higher thickness for a longer period of time. At this time, there is an increased interaction between the plasma and the film surface. Longer interactions happen in the plasma atmosphere, which is how the voluminous cleavage-type structures are made.

3.3. EDX Analyses

PPNVP thin film compositions were analyzed using an EDX attached to a FESEM. Fig. 5 shows the EDX spectra of PPNVP thin films. The mass (%) of constituent elements of the NVP monomer and PPNVP thin films are documented in Table 3. It is found that the PPNVP thin films can be categorized according to three different elements, namely carbon (C), nitrogen (N), and oxygen (O), in spite of the fact that the NVP monomer consists of carbon (C), nitrogen (N), oxygen (O), and hydrogen (H). The primary limitation of EDX involves its lack of ability to identify the existence of elements such as H, He, etc., as it is linked to K-shells that do not correspond to the valence shells.

Table 3 Elements detected by EDX in the NVP monomer and different thickness of PPNVP thin films

Element detected	Mass (%) of NVP (calculated from molecular formula)	Mass (%) of PPNVP thin films		
		209 nm	220 nm	241 nm
C	64.84	5.38	27.47	44.01
N	12.60	0.33	2.99	8.17
O	14.40	44.36	34.64	25.91
H	8.16	Not detected	Not detected	Not detected
Na	-	10.26	7.33	3.59
Mg	-	2.17	1.29	0.92
Al	-	0.69	0.52	0.34
Si	-	31.92	22.21	14.70
Ca	-	4.89	3.55	2.36

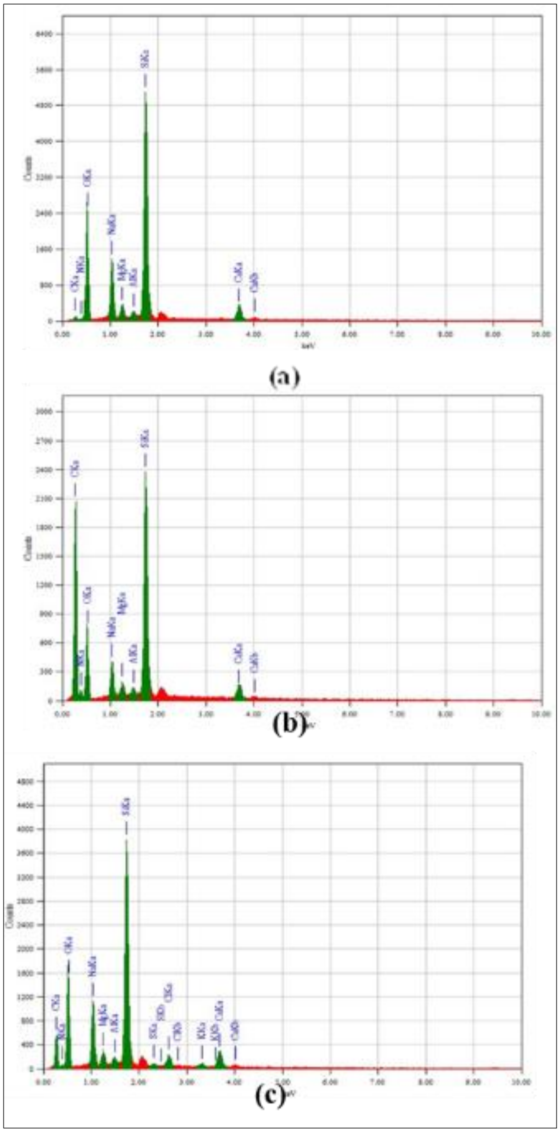

Figure 5 EDX spectra of PPNVP thin films of thicknesses (a) 209 nm, (b) 220 nm, and (c) 241 nm

The EDX analyses indicate that there exists a variation in the mass percentage of the constituents with respect to the thickness of the film. The carbon concentration exhibited a positive correlation with the thickness of the film. The gradual depletion of hydrogen in PPNVP thin films during the plasma process may also account for this observation. The gradual depletion of hydrogen in PPNVP thin films during the plasma process may also account for this observation. In addition to the elemental constituents of the monomer, there are various elements such as Na, Mg, Al, Si and Ca that are also present. The mentioned extra elements may originate from the glass substrates or possibly come from some other discovered source. As the thickness of the film increases, there is a decrease in the proportion of unwanted elements.

3.4. UV-Vis Spectroscopy Analyses

We used UV-Vis spectroscopy to look into the PPNVP thin films' optical properties. The films were less dense at room temperature in the absorbance mode in the 200–1100 nm wavelength range. For PPNVP thin films of different thicknesses, Fig. 6 shows how absorbance (A) changes with λ. The A increases sharply in the ultraviolet region from a low value to a maximum value, showing a peak at around λ= 300 nm, and then reduces exponentially in the visible region of wavelength. At 700 nm, it almost reaches saturation. The maximum A, which corresponds to the wavelength (λmax) of the films for different thicknesses, is listed in Table 4. The intensity of maximum absorbance (Amax) increases with the increase of film thickness, and the peak position shifts to the lower wavelength region. The peaks obtained in the spectra may be due to n–π*. This trend may be attributed to the rise in carbon content or the increase in scattering as the thickness increases.

The optical transmittance, T, of the PPNVP thin films was obtained from absorbance data using the relation $T\ (\%) = \frac{1}{e^{\alpha d}}$. T of the films with varying thicknesses is presented in Fig. 7. All films exhibit a minimum transmittance value at a wavelength of 330 nm. The transmittance of the films increases gradually with the increase of wavelength from 330 nm to 700 nm up to 85% and then approaches a relatively constant value around 90% at λ more than 800 nm. Therefore, we can conclude that the films demonstrate a high level of transparency in the visible spectrum. The data suggests that there is a correlation between thickness and transmittance, whereby an increase in thickness results in a decrease in transmittance. A higher cross-linked density within the material can explain this phenomenon [13].

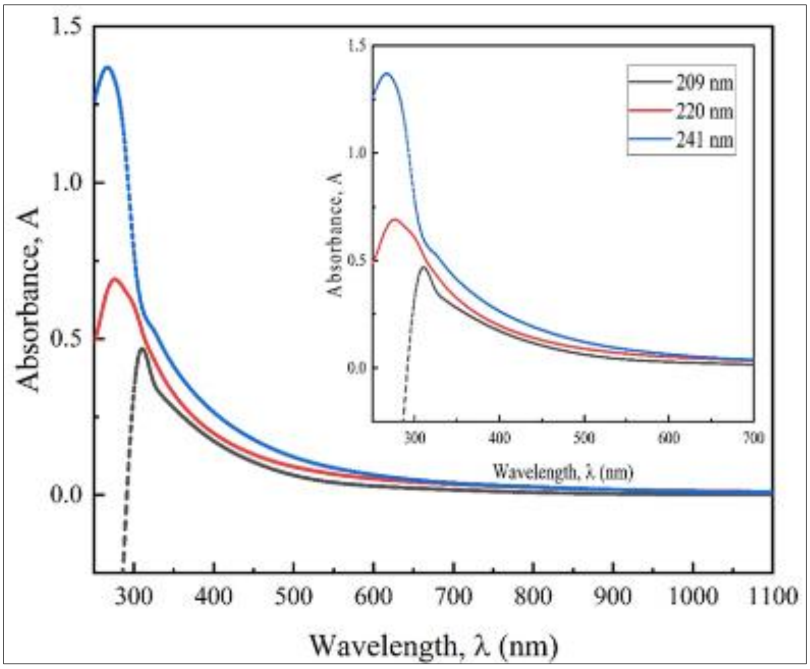

Figure 6 Spectral distribution of absorbance, A at different thicknesses of PPNVP thin films as a function of wavelength

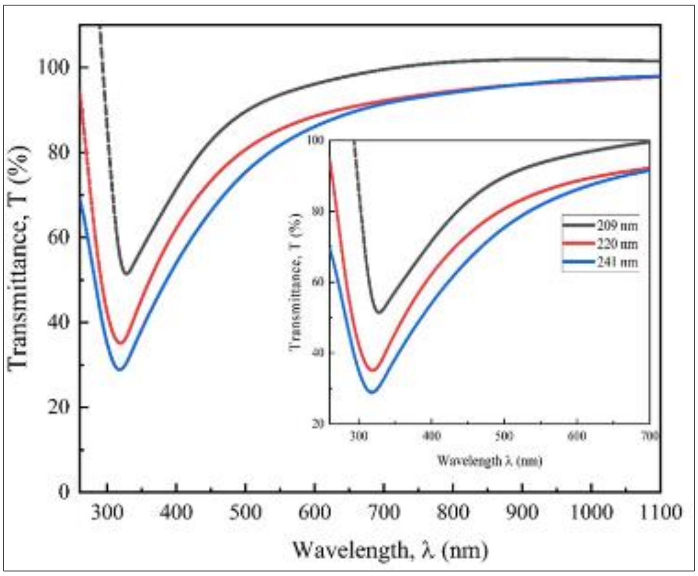

Figure 7 Spectral distribution of transmittance, T (%) at different thicknesses of PPNVP thin films as a function of wavelength

Table 4 Maximum absorbance (Amax) corresponding to the wavelength (λmax) for different thicknesses of the films

Film thickness, d (nm)	Amax	λmax (nm)
209	0.46	310
220	0.69	274
241	1.37	267

The Tauc equation αhν = B(hν - Eg)m was employed to estimate the direct and indirect band gap energies, denoted as Eg(d) and Eg(i), respectively, of the PPNVP thin films. Fig. 8 and Fig. 9 illustrate the variation of (αh𝜈)2 and (αh𝜈)1/2, respectively, within the relation of h𝜈. These figures can be utilized to calculate Eg(d) and Eg(i). The changes that occurred in Eg(d) and Eg(i) with respect to the thickness of the films are presented in Table 5.

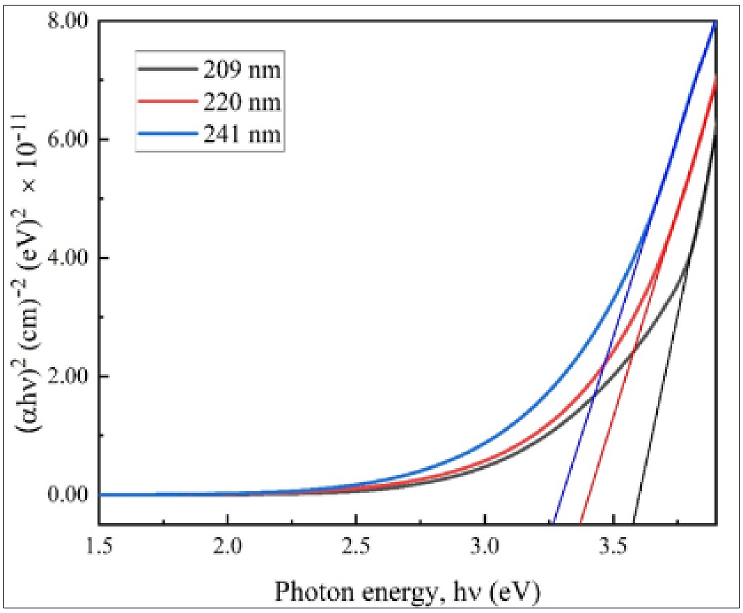

Figure 8 Variation of (αh𝜈)2 vs energy, h𝜈 for different thicknesses of PPNVP thin films

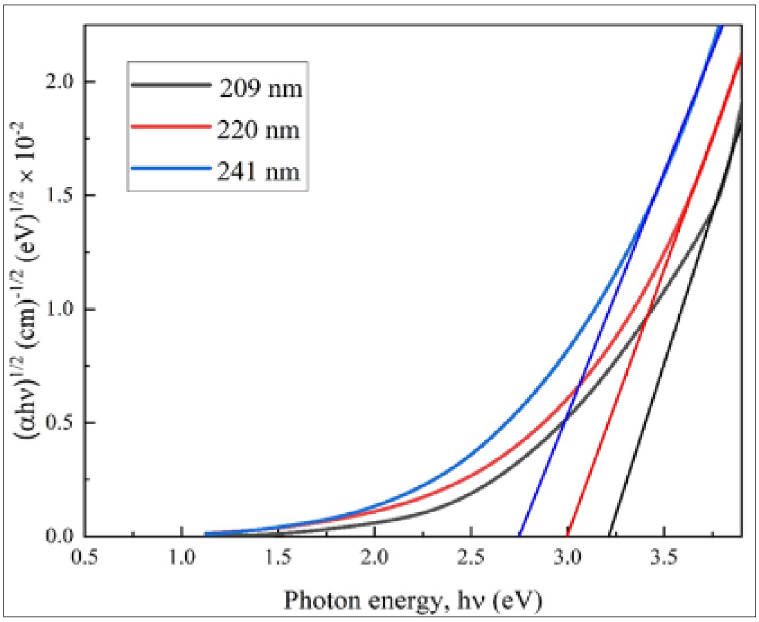

Figure 9 Variation of (αhν)1/2 vs energy, hν for different thicknesses of PPNVP thin films

It is seen from Table 6 that a slight decrease in the values of both Eg(d) and Eg(i) for the deposited films as their thicknesses increased. The decrease in the values of Eg(d) and Eg(i) can be explained as structural defects that arise during the plasma polymerization process [6, 14]. The estimated values of both Eg(d) and Eg(i) for the as-synthesized PPNVP films drop within the range of 3.60–3.30 eV and 3.21–2.75 eV, respectively. These values indicate that the PPNVP thin films have an amorphous or non-crystalline nature [6].

Table 5 Direct band gap Eg(d) and indirect band gap Eg(i) of PPNVP thin films of various thicknesses

Film thickness, d (nm)	**Eg(d) (eV)**	**Eg(i) (eV)**
209	3.60	3.21
220	3.40	2.99
241	3.30	2.75

4. Conclusion

The study of the structural and optical properties of the PPNVP thin films result in significant findings regarding the impact of film thickness. The FTIR spectra of PPNVP thin films exhibit a unique hydrogen bonds peak at around 3660 cm^{-1} corresponds to the stretching vibrations of N–H and O–H. The peak observed at 1250 cm^{-1} represents the C–N stretching vibration, while the peak observed at 2980 cm^{-1} corresponds to the C–H stretching vibration. As the thickness of PPNVP thin films increases, there is a small but notable rise in C–H stretching (2980–2982 cm^{-1}) and a minor decline in C–H bending (1462–1460 cm^{-1}). Characteristic peaks like as C–H bending, C≡N stretching and C=C bending are observed in PPNVP thin films that are absent in conventional polymer techniques.

FESEM micrograph on the PPNVP thin films shows that there is a significant amount of cleavage-type fracture present, which increases with film thicknesses. This indicates the hydrophilic functional groups present in the PPNVP films during deposition. The EDX displays the presence of oxygen, carbon, and nitrogen in this thin film. The concentrations of the elements are varied with respect to the film thickness.

The PPNVP thin films exhibit a high transmittance about 80% in the visible region. As the thickness of the film increases, the direct and indirect band gaps are decreased from 3.60 to 3.30 eV and from 3.21 to 2.75 eV, respectively as become narrower. These findings contribute to a deeper understanding of the relationship between film thickness and the structural, morphological, and optical properties of PPNVP thin films, highlighting their potential applications in optoelectronic devices.

Compliance with ethical standards

Acknowledgments

The authors would like to thank Dhaka University of Engineering & Technology (DUET), Gazipur, Bangladesh, for partially funding this study.

Disclosure of conflict of interest

The authors declare that they have no conflict of interest.

References

[1] H. Yasuda, Plasma Polymerization, Orlando, Florida: Academic Press, Inc., 1985.

[2] T. Afroze and A. H. Bhuiyan, "Electrical conduction mechanism in plasma polymerized 2-(diethylamino)ethyl methacrylate thin films," Polym. Eng. Sci., vol. 55, no. 12, pp. 2729–2734, 2015.

[3] S. Majumder and A. H. Bhuiyan, "Effect of Heat Treatment on the Optical Properties of Plasma-Polymerized Vinylene Carbonate Thin Films," Adv. Polym. Technol., vol. 34, no. 1, pp. 21468 (1–8), 2015.

[4] H. Akther and A. H. Bhuiyan, "Infrared and ultra violet-visible spectroscopic investigation of plasma polymerized N, N, 3, 5-tetramethylaniline thin films," Thin Solid Films, vol. 474, no. 1–2, pp. 14–18, 2005.

[5] R. Matin and A. H. Bhuiyan, "Electrical transport mechanism in plasma polymerized 2, 6, diethylaniline thin films," Thin Solid Films, vol. 519, no. 11, pp. 3462–3467, 2011.

[6] H. Kabir, M. M. Rahman, K. M. Uddin, and A. H. Bhuiyan, "Structural, morphological, compositional and optical studies of plasma polymerized 2-furaldehyde amorphous thin films," Appl. Surf. Sci., vol. 423, pp. 983–994, 2017.

[7] R. E. Marchant, D. Yu, and C. Khoo, "Preparation and characterization of plasma-polymerized N-vinyl-2-pyrrolidone films," J. Polym. Sci.: Part A Polym. Chem., vol. 27, no. 3, pp. 881–895, 1989.

[8] S. Mallakpour and E. Khadem, "Novel poly(N-vinyl-2-pyrrolidone) nanocomposites containing poly(amide–imide)/aluminum oxide nanostructure hybrid as a filler," High Perform. Polym., vol. 28, no. 1, pp. 55–63, 2016.

[9] A. M. Parambil, Y. M. Puttaiahgowda, and P. Shanka, "Copolymerization of N-Vinyl pyrrolidone with methyl methacrylate by Ti(III)-DMG redox initiator," Turkish J Chem., vol. 36, no. 3, pp. 397–409, 2012.

[10] I. Washio, Y. Xiong, Y. Yin, and Y. Xia, "Reduction by the End Groups of Poly(vinyl pyrrolidone): A New and Versatile Route to the Kinetically Controlled Synthesis of Ag Triangular Nanoplates," Adv. Mater., vol. 18, no. 13, pp. 1745–1749, 2006.

[11] X. Liu, Y. Xu, Z. Wu and H. Chen, "Poly(N-vinylpyrrolidone)-Modified Surfaces for Biomedical Applications," Macromol. Biosci, vol. 13, no. 2, pp. 147–154, 2013.

[12] .Muralter, A. Perrotta, and A. Coclite, "Thickness-dependent swelling behavior of vapor-deposited smart polymer thin films," Macromolecules, vol. 51, no. 23, pp. 9692–9699, 2018.

[13] I. Bae, C. Jung, S. Cho, Y. Song, and J. Boo, "A comparative study of plasma polymerized organic thin films on their electrical and optical properties," J. Alloy. Compound., vol. 449, no. 1–2 , pp. 393–396, 2008.

[14] H. Kabir, R. Nasrin, M. M. Rahman, and A. H. Bhuiyan, "Heat treatment effect on the structural, morphological, and optical properties of plasma polymerized furan-2-carbaldehyde thin films," Res. Phys., vol. 16, pp. 103014 (1–10), 2020